ISSN 2663-9092 (Online)

Ukrainian Neurosurgical Journal

Том 32, №3, 2026

Науково-практичний журнал (спеціалізоване видання для лікарів)
Заснований у квітні 1995 року. Виходить 4 рази на рік.
Свідоцтво про державну реєстрацію КВ №23771-13611ПР від 14 лютого 2019 р.

Журнал входить до Переліку наукових фахових видань України, в яких можуть бути опубліковані результати дисертаційних робіт на здобуття наукових ступенів доктора наук, кандидата наук та ступеня доктора філософії (Наказ МОН України від 10.12.2024 № 1721)
Ідентифікатор у Реєстрі суб'єктів у сфері медіа: R40-07048.
Журнал включено до наукометричної бази Scopus.

Всі рукописи, що надходять до редакції, обов'язково рецензуються

Засновники
Інститут нейрохірургії ім. акад. А.П. Ромоданова НАМН України
Українська Асоціація Нейрохірургів
Національна академія медичних наук України

Видавець
Інститут нейрохірургії ім. акад. А.П. Ромоданова НАМН України

Адреса видавця та редакції
вул.Платона Майбороди, 32, Київ, 04050, Україна
Тел. +380 44 483-91-98
Факс +380 44 489-35-61
E-mail: unj.office@gmail.com
http://theunj.org

Підписано до публікації
з оригінал-макета 25.09.2026

Головний редактор
Педаченко Євгеній Георгійович • *Київ, Україна*

Заступник головного редактора
Білошицький Вадим Васильович • *Київ, Україна*

Заступник головного редактора
Васюта Віра Анатоліївна • *Київ, Україна*

Завідувач редакції
Никифорова Анна Миколаївна • *Київ, Україна*

Редакційна колегія
Армонда Рокко А. • *Вашингтон, Сполучені Штати*
Арраез Мігель А. • *Малага, Іспанія*
Валадка Алекс Б. • *Даллас, Сполучені Штати*
Вукич Мирослав • *Загреб, Хорватія*
Гаврилюк Грегорі В. Дж. • *Клівленд, Сполучені Штати*
Газіоглу Нурпері • *Істанбул, Туреччина*
Гук Андрій Петрович • *Київ, Україна*
Ендрюс Рассел Дж. • *Лос Гатос, Сполучені Штати*
Зельман Володимир • *Лос-Анджелес, Сполучені Штати*
Земскова Оксана Володимирівна • *Київ, Україна*
Калангу Казаді • *Хараре, Зімбабве*
Карієв Гайрат Маратович • *Ташкент, Узбекистан*
Като Йоко • *Тойоаке, Японія*
Крегг Роман • Лондон, Велика Британія
Малишева Тетяна Андріївна • *Київ, Україна*
Медведєв Володимир Вікторович • *Київ, Україна*
Меламед Ізраїль • *Беер Шева, Ізраїль*
Нетлюх Андрій Михайлович • *Львів, Україна*
Райнов Микола • *Мюнхен, Німеччина*
Расуліч Лукас Грюіца • *Белград, Сербія*
Розуменко Володимир Давидович • *Київ, Україна*
Рутка Джеймс • *Торонто, Канада*
Сірко Андрій Григорович • *Дніпро, Україна*
Смоланка Володимир Іванович • *Ужгород, Україна*
Смрчка Мартін • *Брно, Чеська Республіка*
Фіщенко Яків Віталійович • *Київ, Україна*
Шлобін Натан А. • *Нью-Йорк, Сполучені Штати*
Хижняк Михайло Віталійович • *Київ, Україна*
Цимбалюк Віталій Іванович • *Київ, Україна*

Оригінал-макет журналу затверджений і рекомендований до друку та поширення через Інтернет на спільному засіданні Редакційної колегії Ukrainian Neurosurgical Journal та вченої ради Інституту нейрохірургії ім. акад. А.П. Ромоданова НАМН України (протокол №12 від 25.09.2026)

Відповідальність за зміст рекламних матеріалів несе рекламодавець

Усі права стосовно опублікованих статей належать їх авторам

Усі права стосовно будь-яких інших публікацій, крім авторських статей, належать видавцеві

Видання використовує ліцензію Creative Commons - CC BY - Зазначення Авторства - https://creativecommons.org/licenses/by/4.0/.
Ця ліцензія дозволяє іншим розповсюджувати, редагувати твір, вносити в нього зміни, і брати його за основу для інших творів, навіть для використання з комерційною метою, за умови зазначення авторства.

Перша сторінка обкладинки

Рисунок до статті Vladyslav I. Kaliuzhka, Mykyta A. Markevych, Mark I. Hlukhenkii, Iurii O. Babalian, Volodymyr O. Piatykop "Endoscopic evacuation of intracerebral hemorrhage using mixed reality navigation: case report", стор. 123-126

Зміст

Оглядова стаття

Yuliia G. Serhiienko, Natalia O. Nekrasova, Yurii O. Kotlyarevskyi, Olena K. Riznychenko, Volodymyr O. Yurko
Endothelial dysfunction as a predictor of post-reperfusion complications in acute ischemic stroke: a literature review 3-9

Ю.В. Фломін, А.Л. Орловська, А.В. Грицан, М.В. Гуляєва, М.Я. Романишин, А.В. Гончар, І.Р. Гаврилів, М.Г. Царяпкін
Порушення ходьби при неврологічних захворюваннях: клінічне значення, методи оцінювання та можливості реабілітації 10-18

В.Ю. Молотковець, В.В. Кондратюк, М.Ю. Побут
Супрамаксимальна резекція гліобластом: від патофізіологічного обґрунтування до клінічної стандартизації 19-27

Оригінальна стаття

Yaroslav D. Bondarenko, Oksana I. Kauk, Iryna O. Hovbakh, Lidiya V. Cherkashyna, Olena K. Riznychenko
A unified mechanism of cross-modal neuroplasticity: hub-based architecture, neurochemical and epigenetic regulation in sensory compensation and synesthesia 28-42

Giussepe Condori-Jara, Jose Acha-Sanchez, Jose Amado-Tineo
Predictive value of the Glasgow Coma Scale for postoperative functional outcomes in patients with aneurysmal subarachnoid hemorrhage: a retrospective study (2018–2021) 43-52

Artem V. Rozumenko, Valentyn M. Kliuchka, Olexandr M. Lisianyi, Oleg O. Dyma, Tetyana A. Malysheva, Volodymyr D. Rozumenko
A ventricular-wall topographic classification for periventricular high-grade gliomas: corridor selection and early surgical outcomes—a pilot single-center series 53-61

М.О. Зорін
25-річний досвід пункційної вертебропластики 62-68

М. Ю. Глухенький, М. В. Каджая, О. С. Готін, А. П. Гук
Краніопластика в проміжний післяопераційний період після вогнепального поранення головного мозку: клінічні та організаційні аспекти своєчасного втручання 69-82

А.М. Дубровка, В.О. Федірко
Інтраопераційні знахідки причин рецидиву болю після мікросудинної декомпресії при невралгії трійчастого нерва: досвід ревізійних втручань 83-92

О.В. Гузун, О.С. Задорожний, Н.В. Коновалова, В.А. Васюта
Неоваскулярна глаукома як хронічна нейроішемічна оптична нейропатія: вплив лікувального навантаження на зір-асоційовану якість життя (36-місячне проспективне дослідження) 93-101

Vladyslav I. Kaliuzhka, Mykyta A. Markevych, Volodymyr K. Klochkov, Volodymyr Y. Prokopiuk, Volodymyr O. Piatykop
Intrathecal cerium oxide nanoparticles improve functional recovery after experimental subarachnoid hemorrhage: a proof-of-concept study 102-115

Н.О. Михайловська, Я.П. Зінькевич, К.Р. Костюк
Аналіз ефективності глибинної стимуляції субталамічних ядер у пацієнтів із розгорнутими стадіями хвороби Паркінсона: український досвід однорічного спостереження 116-122

Спостереження з практики

Vladyslav I. Kaliuzhka, Mykyta A. Markevych, Mark I. Hlukhenkii, Iurii O. Babalian, Volodymyr O. Piatykop
Endoscopic evacuation of intracerebral hemorrhage using mixed reality navigation: case report 123-126

Anh Quynh Dang, Thuy Thi Hong Le, Hung Phi Nguyen, Huyen Thi Tran, Tuan Quoc Nguyen, Vy Thuc Nguyen, Phung Thi Kim Le, Nguyet Le Nhu Dang, Phi Duong Nguyen
Spinal neurocysticercosis: a rare and challenging diagnosis in imaging 127-132

Original article

Ukrainian Neurosurgical Journal. 2026;32(3):102-115
doi: 10.25305/unj.361688

Intrathecal cerium oxide nanoparticles improve functional recovery after experimental subarachnoid hemorrhage: a proof-of-concept study

Vladyslav I. Kaliuzhka [1,2], Mykyta A. Markevych [2], Volodymyr K. Klochkov [3], Volodymyr Y. Prokopiuk [4], Volodymyr O. Piatykop [1,2]

[1] Department of Neurology and Neurosurgery, Kharkiv National Medical University, Kharkiv, Ukraine
[2] Neurosurgery Department, Kharkiv Regional Clinical Hospital, Kharkiv, Ukraine
[3] Yu.V. Malukin Nanostructured Materials Department, Institute for Scintillation Materials National Academy of Sciences of Ukraine, Kharkiv, Ukraine
[4] Department of Cryobiochemistry, Institute for Problems of Cryobiology and Cryomedicine of the National Academy of Sciences of Ukraine, Kharkiv, Ukraine

Received: 25 May 2026
Accepted: 30 June 2026

Address for correspondence:
Vladyslav I. Kaliuzhka, Department of Neurology and Neurosurgery, Kharkiv National Medical University, 4 Nauky avenue, Kharkiv, 61022, Ukraine.
email: vladislavkalyuzhka@gmail.com

Background: Early brain injury following aneurysmal subarachnoid hemorrhage (SAH) is driven by oxidative stress, neuroinflammation, microvascular dysfunction, and neuronal damage. Cerium oxide nanoparticles (CeO_2 nanoparticles) possess regenerative antioxidant properties and may provide sustained scavenging of reactive oxygen species. This proof-of-concept study evaluated whether intrathecal administration of CeO_2 nanoparticles improved functional recovery after experimental SAH.

Methods: Thirty adult male rats were randomly allocated to three groups: Sham, SAH with conventional nimodipine treatment, and SAH with intrathecal CeO_2 nanoparticle treatment (n = 10 per group). SAH was induced using the endovascular perforation model. One hour after SAH induction, animals received intrathecal CeO_2 nanoparticles at 0.5 mg/kg, conventional nimodipine at 0.05 mg/kg, or an equivalent volume of saline. Neurological function was assessed using the modified Garcia score and beam balance test. Spontaneous locomotor and exploratory activity was evaluated using automated open-field video tracking. Body weight and survival were monitored throughout the 21-day observation period.

Results: Intrathecal CeO_2 nanoparticle treatment was associated with significantly improved longitudinal neurological and behavioral recovery compared with conventional nimodipine treatment. On day 21, the nanotherapy group demonstrated higher modified Garcia scores (17.00 vs 14.83; adjusted $p = 0.002$) and beam balance scores (5.60 vs 4.63; adjusted $p = 0.002$). Nanotherapy also improved travelled distance (4153.88 vs 3743.00 cm; adjusted $p < 0.001$), mean locomotor velocity (13.86 vs 12.48 cm/s; adjusted $p < 0.001$), and center exploration (41.35 vs 37.73s; adjusted $p < 0.001$), while reducing immobility time (40.76 vs 54.17s; adjusted $p = 0.002$). Survival at the end of follow-up was 100% in the Sham group, 60% in the Conventional treatment group, and 80% in the Nanotherapy group; however, the difference between active treatment groups was not statistically significant.

Conclusions: Intrathecal administration of cerium oxide nanoparticles improved neurological function, motor coordination, spontaneous locomotor activity, exploratory behavior, and general postoperative recovery after experimental SAH. These findings provide proof-of-concept evidence supporting nanoceria as a potential local antioxidant therapy for early brain injury after SAH. Further studies should assess dose-response relationships, safety, pharmacokinetics, histopathological effects, and molecular mechanisms of neuroprotection.

Keywords: *subarachnoid hemorrhage; cerium oxide nanoparticles; nanoceria; intrathecal administration; oxidative stress; neurological recovery; open-field test; early brain injury*

Introduction

Aneurysmal subarachnoid hemorrhage (aSAH) remains one of the most devastating forms of stroke, accounting for approximately 5% of all cerebrovascular events while disproportionately affecting younger and middle-aged individuals. Despite advances in microsurgical clipping, endovascular aneurysm occlusion, neurocritical care, and multimodal monitoring, mortality remains between 25% and 40%, whereas nearly half of survivors experience persistent neurological disability, cognitive impairment, or reduced quality of life. Consequently, aSAH imposes a substantial socioeconomic burden due to long-term disability among working-age individuals. Although prevention of aneurysm rebleeding has improved markedly over the last decades, secondary brain injury continues to represent the principal determinant of neurological outcome.

Traditionally, delayed cerebral vasospasm was considered the primary mechanism responsible for poor neurological recovery after aSAH. However, increasing

Copyright © 2026 Vladyslav I. Kaliuzhka, Mykyta A. Markevych, Volodymyr K. Klochkov, Volodymyr Y. Prokopiuk, Volodymyr O. Piatykop

This work is licensed under a Creative Commons Attribution 4.0 International License
https://creativecommons.org/licenses/by/4.0/

experimental and clinical evidence has fundamentally changed this concept [1]. Current understanding recognizes aSAH as a biphasic disease consisting of early brain injury (EBI), occurring within the first 72 hours after hemorrhage, followed by delayed cerebral ischemia (DCI), which develops several days later. Numerous studies have demonstrated that neurological outcome correlates more closely with the severity of early brain injury than with angiographic vasospasm alone, emphasizing the importance of neuroprotective strategies targeting the acute phase following aneurysm rupture.

Early brain injury represents a complex cascade initiated immediately after arterial rupture. The abrupt accumulation of blood within the subarachnoid space produces a rapid elevation of intracranial pressure, transient global cerebral ischemia, impaired cerebral autoregulation, blood-brain barrier disruption, microvascular dysfunction, mitochondrial injury, and widespread activation of inflammatory signaling pathways [2]. These interconnected events result in neuronal apoptosis, cerebral edema, endothelial dysfunction, and progressive neurological deterioration even before the onset of angiographic vasospasm.

Among the multiple mechanisms contributing to EBI, oxidative stress has emerged as one of the central mediators of secondary brain damage. Hemoglobin degradation products released into the subarachnoid space catalyze the excessive formation of reactive oxygen species (ROS), including superoxide anions, hydroxyl radicals, and hydrogen peroxide. Under physiological conditions, endogenous antioxidant systems effectively maintain redox homeostasis [3]. Following aSAH, however, the massive oxidative burst rapidly overwhelms intrinsic antioxidant defenses, resulting in lipid peroxidation, protein oxidation, mitochondrial dysfunction, DNA damage, and activation of apoptotic pathways. Oxidative stress further amplifies neuroinflammation through the activation of microglia, endothelial cells, and infiltrating leukocytes, thereby establishing a self-perpetuating cycle of neuronal injury.

Neuroinflammation represents another hallmark of secondary injury after subarachnoid hemorrhage. Blood degradation products activate resident microglia and astrocytes, leading to the production of pro-inflammatory cytokines, chemokines, adhesion molecules, and matrix metalloproteinases. These mediators contribute to blood-brain barrier disruption, leukocyte recruitment, cerebral edema, and delayed neuronal degeneration. Importantly, increasing evidence suggests that oxidative stress and neuroinflammation are tightly interconnected processes rather than independent pathological mechanisms. Reactive oxygen species stimulate inflammatory signaling pathways, whereas inflammatory cells further increase oxidative stress, creating a vicious cycle that exacerbates neurological injury.

Currently, oral nimodipine remains the only pharmacological therapy consistently recommended by international guidelines for patients with aSAH. Its beneficial effect is believed to result primarily from neuroprotective rather than direct vasodilatory properties. Nevertheless, the clinical efficacy of nimodipine remains limited. Systemic administration is associated with variable bioavailability, hypotension, and relatively low drug concentrations within the cerebrospinal fluid. Consequently, considerable interest has focused on alternative delivery strategies capable of increasing local drug concentration while minimizing systemic adverse effects.

Intrathecal drug administration represents a particularly attractive approach for treating diseases involving the subarachnoid space [4-5]. Direct delivery into the cerebrospinal fluid bypasses the blood-brain barrier, allows higher local drug concentrations at the site of injury, prolongs therapeutic exposure, and reduces systemic toxicity. Experimental and early clinical studies investigating intrathecal vasodilators, fibrinolytic agents, and sustained-release nimodipine formulations have demonstrated encouraging results, supporting the concept that local pharmacological intervention may represent an effective strategy for attenuating secondary brain injury following aSAH.

Nanomedicine has recently emerged as a promising therapeutic platform capable of overcoming several limitations of conventional pharmacotherapy [6]. Nanoparticle-based drug delivery systems improve pharmacokinetic profiles, enhance tissue penetration, provide sustained drug release, and enable multifunctional therapeutic approaches combining targeted drug delivery with intrinsic biological activity. Among the various nanomaterials, cerium oxide nanoparticles (CeO_2 nanoparticles, nanoceria) have attracted particular attention because of their unique regenerative antioxidant properties. Unlike conventional antioxidants, nanoceria possess reversible Ce^{3+}/Ce^{4+} redox cycling, enabling continuous scavenging of reactive oxygen species without rapid depletion [7-8]. Consequently, cerium oxide nanoparticles exhibit superoxide dismutase-, catalase-, and peroxidase-like activities, making them potent catalytic antioxidants capable of reducing oxidative damage in multiple neurological disease models.

Experimental studies have demonstrated that cerium oxide nanoparticles attenuate oxidative stress, reduce neuronal apoptosis, suppress neuroinflammatory activation, decrease cerebral edema, and improve neurological recovery following ischemic stroke, traumatic brain injury, and subarachnoid hemorrhage [9]. Importantly, previous investigations have shown that nanoceria improve survival and neurological function after experimental SAH through reduction of oxidative stress and inflammatory injury. These findings suggest that cerium oxide nanoparticles may represent a promising adjunctive therapy capable of targeting the pathological mechanisms responsible for early brain injury.

The present study was designed as a proof-of-concept investigation evaluating the functional efficacy of intrathecal cerium dioxide nanoparticles in a rat model of aSAH induced by endovascular perforation. We hypothesized that local nanotherapeutic intervention would improve neurological recovery, motor performance, sensorimotor integration, exploratory behavior, and postoperative body weight recovery compared with conventional nimodipine treatment. Establishing functional efficacy represents the first step toward subsequent mechanistic studies investigating neuroinflammation, oxidative stress, vascular remodeling, and the histopathological correlates of neuroprotection following experimental subarachnoid hemorrhage.

Materials and methods

Synthesis of the CeO_2 NPs

Cerium chloride heptahydrate $CeCl_3 \cdot 7H_2O$ (99.9%) and sodium citrate $Na_3C_6H_5O_7$ (99%) were obtained from "Acros Organics". Hexamethylenetetramine $(CH_2)_6N_4$, (99%), hydrogen peroxide H_2O_2, (60%), sodium hydroxide NaOH (99%), calcium chloride $CaCl_2$ (98%) and ammonium hydroxide NH_4OH, (25%) from "Macrochem Co. Ltd." were used.

$CeCl_3$ solution (100 mL, 2 mM) was mixed with 100 mL of hexamethylenetetramine solution (4 mM) and stirred using a magnetic stirrer for 3 h at room temperature. Subsequently, 1.8 mL of NH_4OH and 0.6 mL of H_2O_2 were added to the solution. Then, the solution was put in a round-bottom flask and refluxed for 12 h. The solution was evaporated in a rotary evaporator flask under vacuum at the bath temperature of 70 °C to 30 mL. A solution of 2 M $CaCl_2$ was added to the obtained solution until the resulting solution became turbid. Then, the solid phase was precipitated by centrifugation at 7000 rpm for 15 min. The precipitate was separated and a solution of calcium chloride was added again. The procedure of precipitate cleaning was repeated three times. After the last stage of centrifugation, a solution of sodium citrate with a CeO_2/NaCt molar ratio of 1:1 was added to the precipitate. The obtained nanoparticles had an average size of approximately 2 nm. CeO_2 nanoparticles were stabilized by sodium citrate with a molar ratio of 1:1. The solutions were dialyzed for 48 h against deionized water to remove the excess ions and organic species. Dialysis tubing membrane with a molecular weight cutoff of "Cellu Sep H1" 3.5 kDa was used, and water was renewed every 6 h (water/colloid volume ratio = 40). The electrical conductivity of the dialysate was monitored to assess the removal of electrolyte impurities during dialysis. TEM images (***Fig. 1***) revealed the presence of well-defined, nearly monodisperse nanoparticles with an average size of approximately 2 nm. Nanoparticle size was determined using transmission electron microscope JEM-1230 (JEOL, Japan; spatial resolution of 0.2 nm). The physicochemical properties of these cerium oxide nanoparticles have been described previously [10-11].

A glucose solution was added to the aqueous nanoparticle solution. Thus, solutions containing 2 g/L of CeO_2 NPs in a 5% glucose solution were prepared for the experiments.

Study Design

This randomized, controlled experimental study was designed to evaluate the efficacy of intrathecal administration of cerium dioxide nanoparticles in improving functional recovery following experimental aSAH. The primary endpoint was neurological recovery assessed by standardized behavioral tests. Secondary endpoints included locomotor activity, sensorimotor performance, postoperative body weight dynamics, and survival. Histopathological and molecular analyses were intentionally excluded from the present proof-of-concept study and will be presented in subsequent investigations.

Animals

Adult WAG male rats (280–320 g, 10–12 weeks of age) were obtained from Experimental Clinic of Kharkiv National Medical University and acclimatized for seven days before surgery. Animals were housed under controlled environmental conditions (22 ± 2°C, 50–60% humidity, 12-hour light/dark cycle) with unrestricted access to food and water. All procedures complied with the European Directive 2010/63/EU for the protection of animals used for scientific purposes and were approved by the Institutional Ethics Committee.

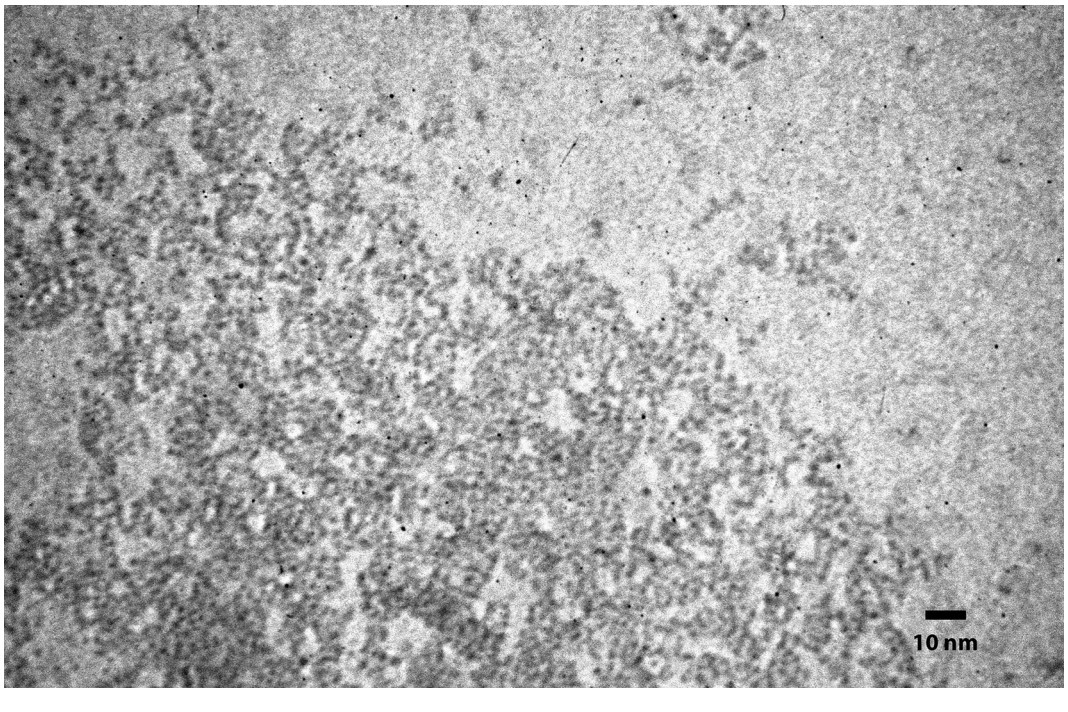


Fig. 1. TEM image of CeO2 nanoparticles

Experimental Groups

Animals were randomly allocated using a computer-generated randomization sequence into three experimental groups: Group 1. Sham-operated animals underwent identical surgical exposure without arterial perforation and received intrathecal sterile saline. Group 2. Animals underwent experimental SAH followed by conventional nimodipine treatment according to the experimental protocol. Group 3. Animals underwent experimental SAH followed by intrathecal administration of cerium dioxide nanoparticles.

Experimental SAH Model

Experimental subarachnoid hemorrhage was induced using the endovascular perforation model [12]. Animals were anesthetized using inhalational isoflurane (4% induction, 2% maintenance). Body temperature was maintained at 37.0 ± 0.5°C using a thermostatically controlled heating pad throughout the procedure. Following a midline cervical incision, the left common carotid artery, external carotid artery, and internal carotid artery were microsurgically exposed. A sharpened 4-0 nylon monofilament was introduced through the external carotid artery stump into the internal carotid artery and advanced to the anterior cerebral artery–middle cerebral artery bifurcation. The vessel wall was perforated by advancing the filament approximately 3 mm beyond the point of resistance, after which the filament was immediately withdrawn to induce subarachnoid hemorrhage. Animals in the sham group underwent identical surgical exposure without arterial perforation.

Intrathecal Treatment

One hour following SAH induction, animals allocated to the nanotherapy group received intrathecal administration of the cerium dioxide (0.5 mg Ce/kg) nanoparticle formulation through cisterna magna puncture. Animals in the Conventional treatment group received intrathecal administration nimodipine therapy according to the experimental protocol (0.05 mg/kg), whereas sham-operated animals received an equivalent volume of sterile physiological saline.

The nanoparticle dose of 0.5 mg/kg was selected as a low-dose local intrathecal regimen intended to provide antioxidant activity within the cerebrospinal fluid while limiting the potential risks of concentration-dependent nanoparticle aggregation and neurotoxicity [9]. Dose selection was informed by previous experimental evidence demonstrating the neuroprotective activity of nanoceria in neurological injury models, including experimental subarachnoid hemorrhage, as well as by the physicochemical characteristics of the citrate-stabilized formulation used in the present study.

Treatment was administered 1 h after SAH induction to target the early phase of brain injury, during which oxidative stress, mitochondrial dysfunction, blood–brain barrier impairment, and inflammatory signaling are initiated. This time point also allowed initial postoperative stabilization of the animals while preserving a clinically relevant early therapeutic window. Because only one dose and one administration time were evaluated, the present study was not designed to establish a dose–response relationship, minimum effective dose, or maximum tolerated dose.

Postoperative Care

Following surgery, animals were placed in temperature-controlled recovery cages until complete recovery from anesthesia. Animals were examined daily for neurological deterioration, hydration status, food intake, wound healing, and body weight. Humane endpoints included persistent inability to obtain food or water, loss of more than 20% body weight, severe neurological deterioration, or moribund condition requiring euthanasia.

Behavioral Assessment

Behavioral testing was performed by investigators blinded to treatment allocation according to the predefined experimental timeline.

Modified Garcia Neurological Score

Global neurological function was evaluated using the modified Garcia neurological scoring system consisting of six domains: spontaneous activity, symmetry of limb movement, forelimb extension, climbing ability, proprioception, and response to vibrissae stimulation [13]. Total scores ranged from 3 to 18, with higher values indicating better neurological performance. Neurological evaluation was performed at baseline and on postoperative days 1, 3, 7, 14, 21.

Beam Balance Test

Motor coordination and balance were assessed using the Beam Balance Test. Animals were placed on a narrow elevated beam, and performance was graded according to a standardized scoring system. Testing was performed on postoperative days 3, 7, 14, 21.

Open Field Test

Spontaneous locomotor activity, exploratory behavior, and anxiety-like behavior were assessed using the Open Field Test. Each rat was placed in the center of a circular open-field arena (200 cm in diameter, opaque walls 40 cm high) and allowed to explore freely for 10 min [14].

Animal behavior was continuously recorded using an overhead high-definition digital camera. Video recordings were analyzed offline using a custom-developed Python-based computer vision pipeline specifically designed for automated behavioral assessment. The analysis software was developed using Python (Python Software Foundation, Wilmington, DE, USA) with computer vision libraries including OpenCV and NumPy (***Fig. 2***).

The tracking algorithm automatically detected the animal in each video frame using background subtraction and contour-based object detection, calculated the centroid position throughout the recording, and reconstructed the locomotor trajectory. Behavioral parameters were subsequently extracted using predefined computational algorithms with identical processing settings applied to all recordings. The following parameters were quantified: Total distance travelled (cm), Mean locomotor velocity (cm/s), center time (s), Immobility time (s). Behavioral videos were processed automatically without manual trajectory correction. Investigators responsible for statistical analysis remained blinded to treatment allocation throughout data processing and outcome assessment. The Open Field Test was performed at baseline and on postoperative days 7 and 21 to evaluate locomotor recovery, exploratory behavior, and anxiety-like behavior following SAH and treatment.

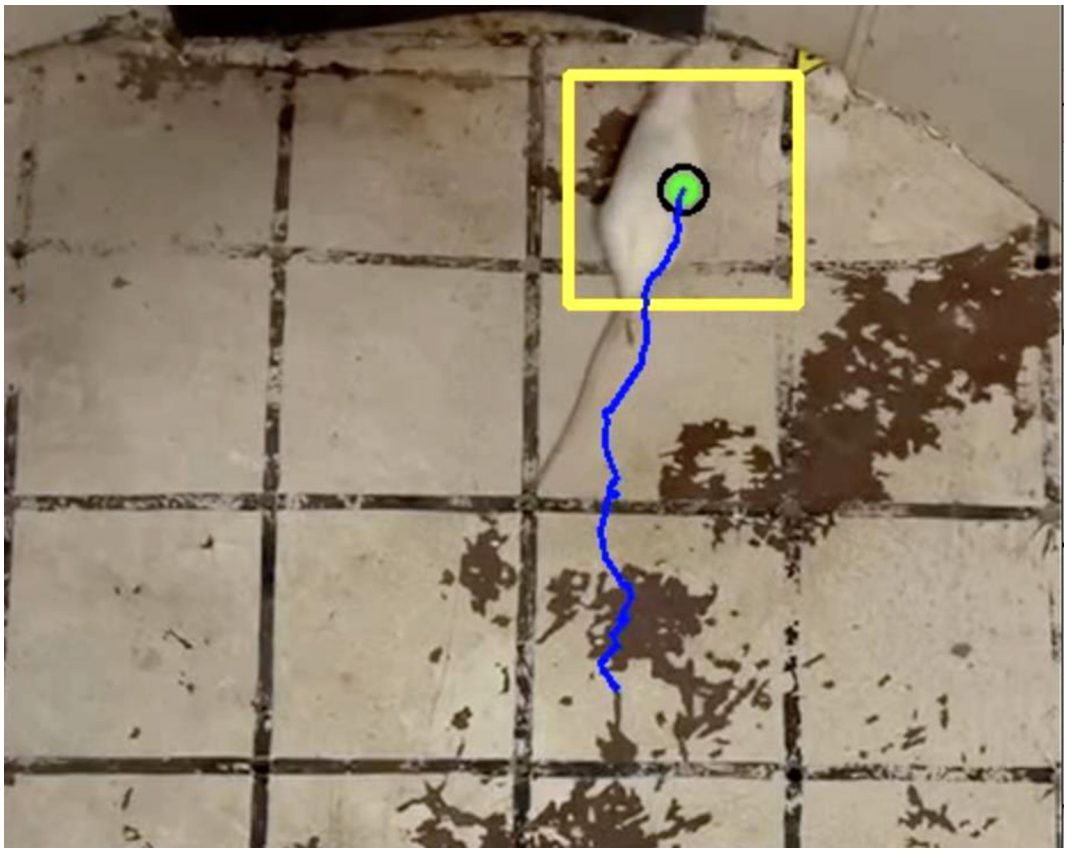


Fig. 2. Representative open-field tracking of a rat. The blue line indicates the animal's locomotor trajectory during the recording period. The yellow square represents the defined region of interest, while the green marker indicates the detected center point of the animal

Body Weight Assessment

Body weight was measured before surgery and subsequently on postoperative days 1, 3, 7, 14, 21, and 28 using a calibrated digital balance. Body weight dynamics were analyzed as an integrated indicator of postoperative recovery, neurological function, nutritional intake, and general health status. Results were expressed as absolute body weight (g).

Survival Analysis

Animals were monitored daily throughout the 28-day observation period. Survival time and mortality were recorded and analyzed using Kaplan–Meier survival curves.

Statistical Analysis

Statistical analyses were performed at the individual animal level using two-sided tests, with $p < 0.05$ considered statistically significant. Continuous variables were summarized as mean ± standard deviation, ordinal outcomes were additionally assessed using rank-based methods, and categorical variables were presented as counts and percentages. Baseline differences among the Sham, the Conventional treatment, and the Nanotherapy groups were evaluated using one-way analysis of variance for continuous variables. Survival was analyzed using Kaplan–Meier curves, with animals surviving to day 28 were censored at the end of follow-up. Pairwise survival differences were assessed using the log-rank test, and mortality proportions were compared using Fisher's exact test. Pairwise p-values were adjusted using the Holm procedure.

Longitudinal outcomes were analyzed using generalized estimating equations with the individual animal specified as the clustering unit to account for repeated measurements. Gaussian models with an identity link, exchangeable working correlation structure, and robust sandwich standard errors included treatment group, time as a categorical factor, and the group-by-time interaction. Baseline values were included as covariates for body weight and open-field outcomes. Modified Garcia and beam-balance scores were analyzed as quasi-continuous longitudinal outcomes because of the limited sample size and restricted score range. Overall longitudinal effects were evaluated using Wald χ^2 tests. Prespecified time-point comparisons between the Nanotherapy and the Conventional treatment groups were performed using Welch's t-test for continuous variables and the Mann–Whitney U test for ordinal scores, with Holm adjustment for multiple comparisons. Effect sizes were reported as Hedges' g and Cliff's delta.

Missing observations after death were treated as structurally missing and were not imputed. No last-observation-carried-forward, zero substitution, or post-death score assignment was applied. All available pre-death observations were included in the longitudinal models, while survival and functional outcomes were interpreted separately because mortality-related dropout may introduce survivor bias. As sensitivity analyses, area-under-the-curve (AUC) values were calculated using the trapezoidal rule among animals with complete follow-up, and associations among day-21

neurological and behavioral outcomes were examined using Spearman's rank correlation.

No formal power calculation was performed because reliable preliminary estimates of the variability of functional outcomes after intrathecal administration of the specific citrate-stabilized CeO_2 formulation were unavailable. A sample size of 10 animals per group was selected as appropriate for an initial proof-of-concept experiment, considering the group sizes used in comparable experimental SAH studies, anticipated model-related attrition, operational feasibility, and the Reduction principle.

Results

Study population, baseline characteristics, and data completeness

A total of 30 rats were included in the final analysis and equally allocated to the Sham, the Conventional treatment, and the Nanotherapy groups, with 10 animals per group (***Fig. 3***). All baseline measurements were complete. The study groups were comparable at baseline with respect to body weight and open-field behavioral parameters. Mean baseline body weight was 312.44 ± 8.68 g in the Sham group, 316.96 ± 2.38 g in the Conventional treatment group, and 313.09 ± 5.66 g in the Nanotherapy group (one-way ANOVA, $p = 0.224$).

No significant baseline differences were observed in distance travelled ($p = 0.904$), mean velocity ($p = 0.858$), center exploration ($p = 0.902$), or immobility time ($p = 0.908$). Baseline modified Garcia and beam-balance scores were identical in all animals, with scores of 18 and 6, respectively.

Post-injury missing observations were predominantly attributable to animal death and followed a monotone dropout pattern. No post-death measurements were imputed.

Survival and mortality

All animals in the Sham group survived throughout the 28-day observation period. Four deaths occurred in the Conventional treatment group, representing a 28-day mortality rate of 40%, whereas the Nanotherapy group demonstrated a lower mortality rate of 20% (two deaths). Deaths in the Conventional treatment group occurred on days 1, 2, 2 and 4, with a median time to death of 2 days. In the Nanotherapy group, deaths occurred on days 2 and 8, with a median death day of 5.

Kaplan–Meier analysis demonstrated numerically higher survival in the Nanotherapy group than in the Conventional treatment group (***Fig. 4***). However, the difference did not reach statistical significance in the pairwise log-rank analysis (unadjusted $p = 0.294$; Holm-adjusted $p = 0.294$). Given the limited sample size and low number of events, the survival findings should be considered exploratory.

Longitudinal body-weight recovery

Body weight changed differently over time among the three study groups (***Fig. 5***). A baseline-adjusted generalized estimating equation model, including 127 post-injury observations from 29 animals, demonstrated a significant group-by-time interaction (Wald $\chi^2[8] = 9198.44$, $p < 0.001$). Animals receiving nanotherapy showed faster and more complete recovery of body weight compared with animals receiving conventional treatment. At day 28, mean body weight was 327.68 ± 9.03 g in the Sham group, 318.43 ± 2.89 g in the Conventional treatment group, and 325.28 ± 6.24 g in the Nanotherapy group. Among surviving animals, the mean difference between the Nanotherapy and Conventional treatment groups at day 28 was 6.84 g, corresponding to a Hedges' g of 1.25. The unadjusted between-group p-value was 0.020, although the difference did not remain statistically significant after Holm correction for multiple time-point comparisons (adjusted $p = 0.061$).

Neurological function

Modified Garcia score

Subarachnoid hemorrhage induced a marked early reduction in neurological performance in both active-treatment groups, followed by progressive recovery (***Fig. 6***). The pattern of recovery differed significantly among groups. The longitudinal generalized estimating equation model included 129 measurements from all 30 animals and demonstrated a significant group-by-time interaction (Wald $\chi^2[8] = 38469.70$, $p < 0.001$).

At day 21, the mean modified Garcia score was 18 ± 0.00 in the Sham group, 14.83 ± 0.41 in the Conventional treatment group, and 17.00 ± 0.00 in the Nanotherapy group. The mean difference between the Nanotherapy and Conventional treatment groups was 2.17 points.

The day-21 difference was statistically significant in the rank-based comparison after adjustment for multiple testing (Holm-adjusted $p = 0.002$). The corresponding standardized effect size was large (Hedges' $g = 7.70$), indicating substantially better neurological recovery in the Nanotherapy group.

Beam-balance score

Beam-balance performance also showed a significant treatment-dependent temporal pattern (***Fig. 7***). The generalized estimating equation analysis included 129 observations from 30 animals and identified a significant group-by-time interaction (Wald $\chi^2[8] = 21956.83$, $p < 0.001$). At day 21, the mean beam-balance score was 6.00 ± 0.00 in the Sham group, 4.63 ± 0.16 in the Conventional treatment group, and 5.60 ± 0.00 in the Nanotherapy group. Nanotherapy was associated with a mean improvement of 0.97 points relative to Conventional treatment. The difference between the two active-treatment groups remained statistically significant after Holm correction (adjusted $p = 0.002$), with a large standardized effect size (Hedges' $g = 8.59$).

Open-field locomotor and exploratory activity

Travelled distance

The temporal trajectory of travelled distance differed significantly among groups (***Fig. 8***). The baseline-adjusted generalized estimating equation model included 99 post-injury observations from 26 animals and demonstrated a significant group-by-time interaction (Wald $\chi^2[6] = 21505.68$, $p < 0.001$). At day 21, the mean travelled distance was 4294.40 ± 110.78 s in the Sham group, 3743.00 ± 125.45 s in the Conventional treatment group, and 4153.88 ± 77.68 s in the Nanotherapy group. Nanotherapy increased travelled distance by a mean of 410.88 s compared with Conventional treatment. This difference remained statistically significant after correction for multiple testing (Holm-adjusted $p < 0.001$) and was associated with a large effect size (Hedges' $g = 3.83$).

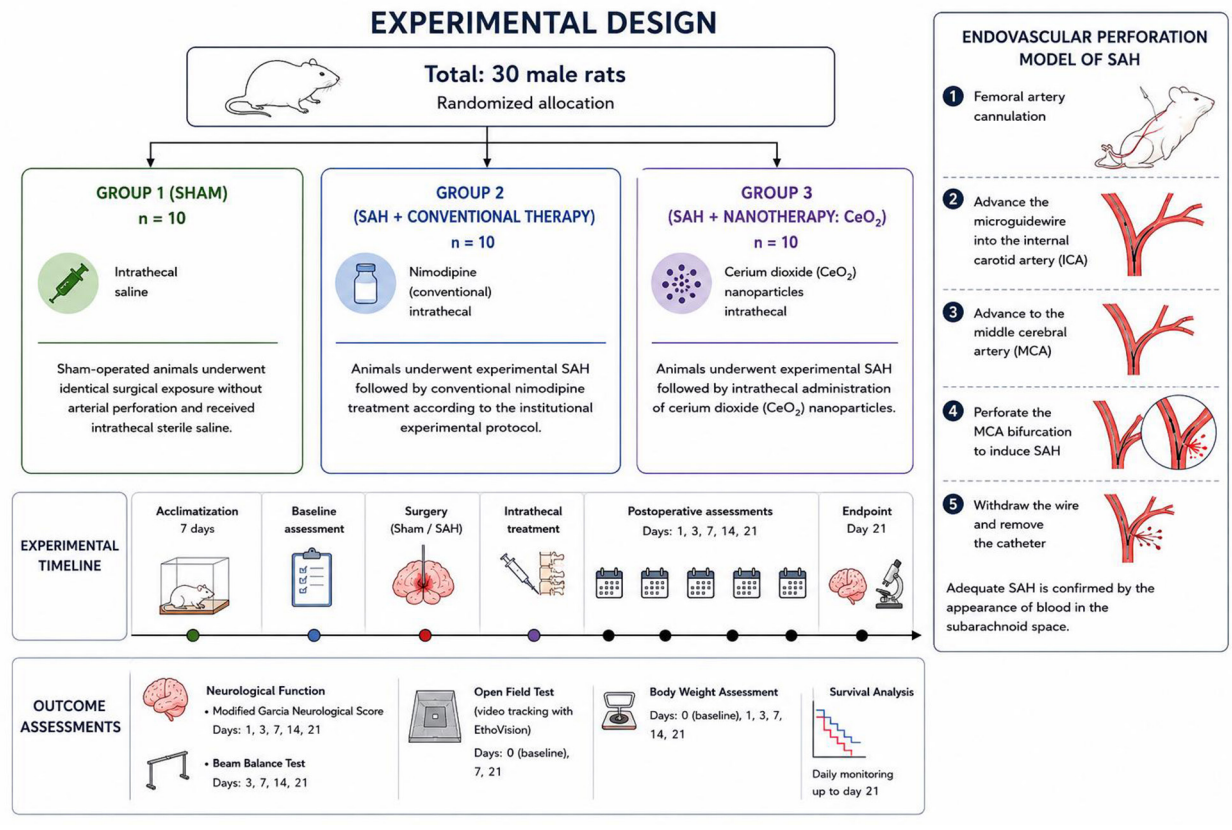


Fig. 3. Experimental design and assessment schedule for the rat model of subarachnoid hemorrhage

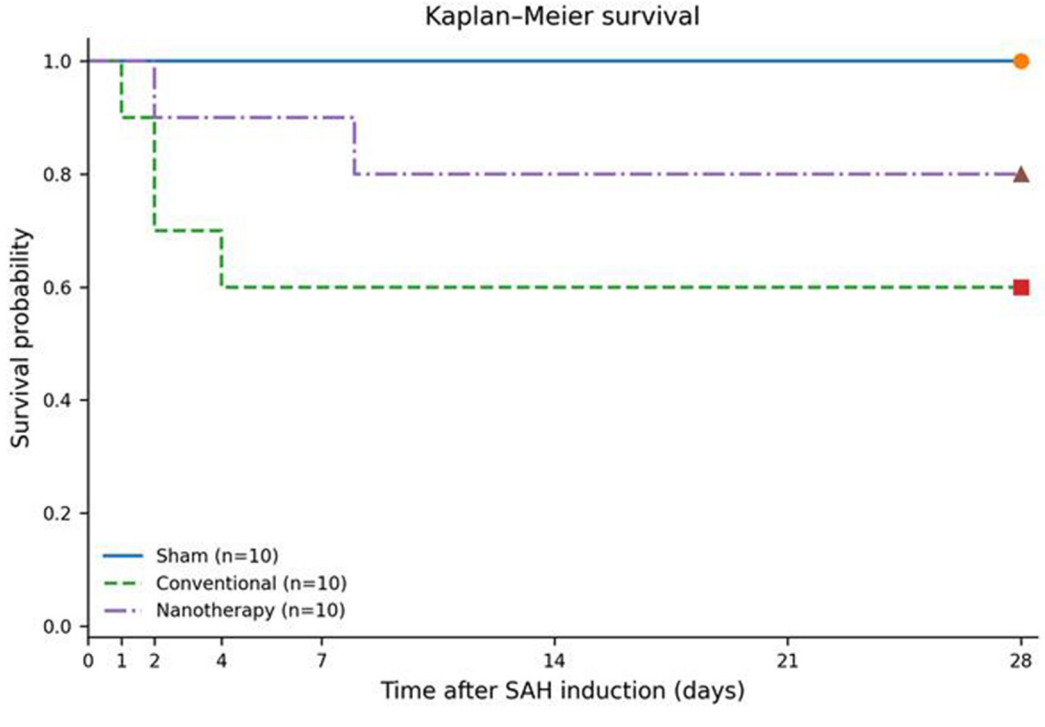


Fig. 4. Kaplan–Meier survival analysis following subarachnoid hemorrhage induction

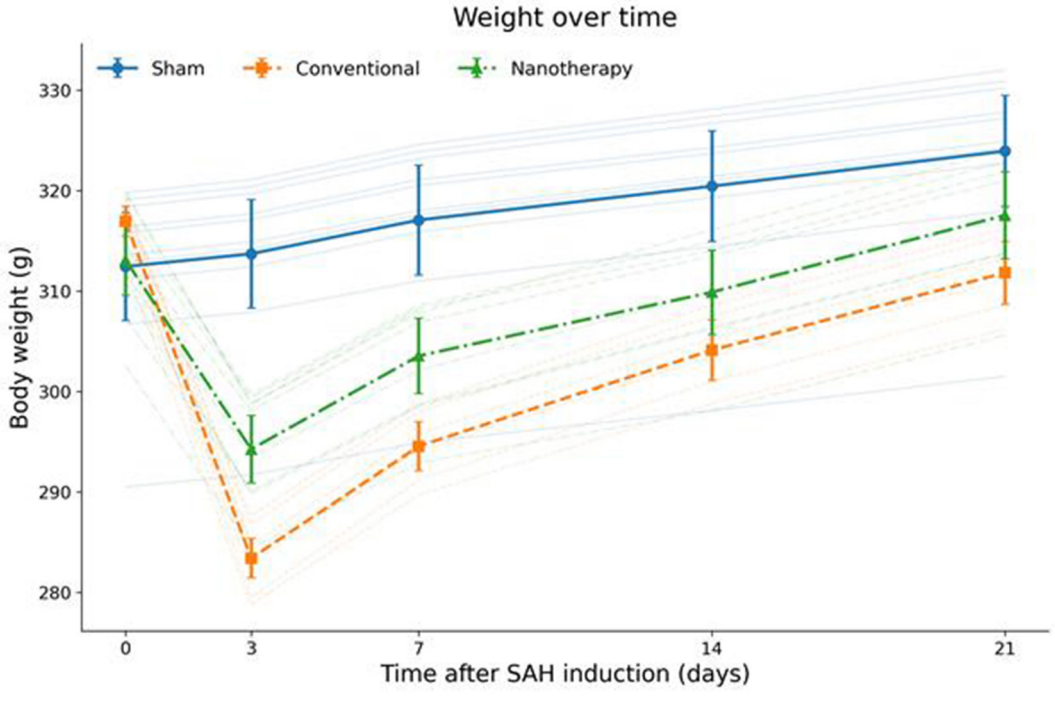


Fig. 5. Changes in body weight following subarachnoid hemorrhage induction

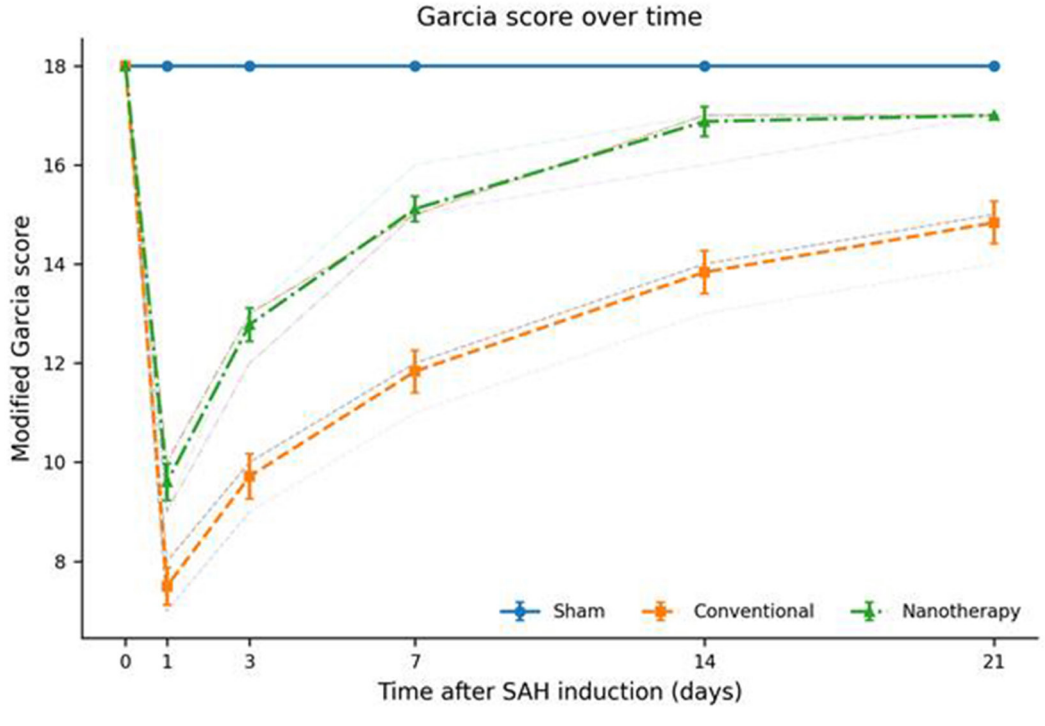


Fig. 6. Changes in neurological function following subarachnoid hemorrhage induction

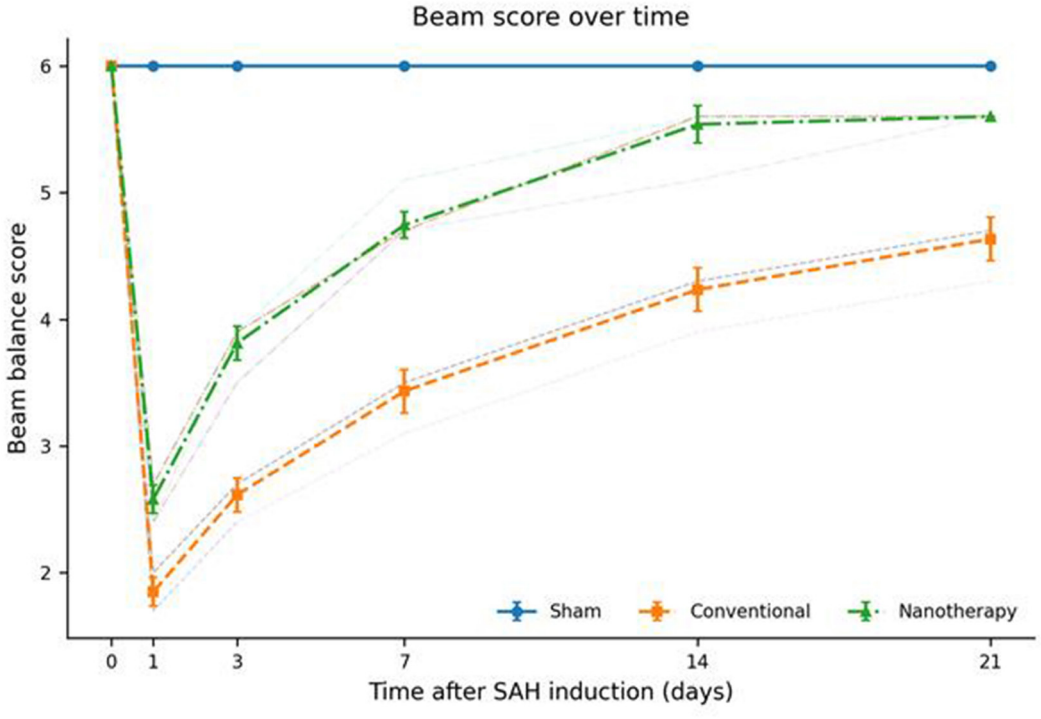


Fig. 7. Changes in beam-balance performance following subarachnoid hemorrhage induction

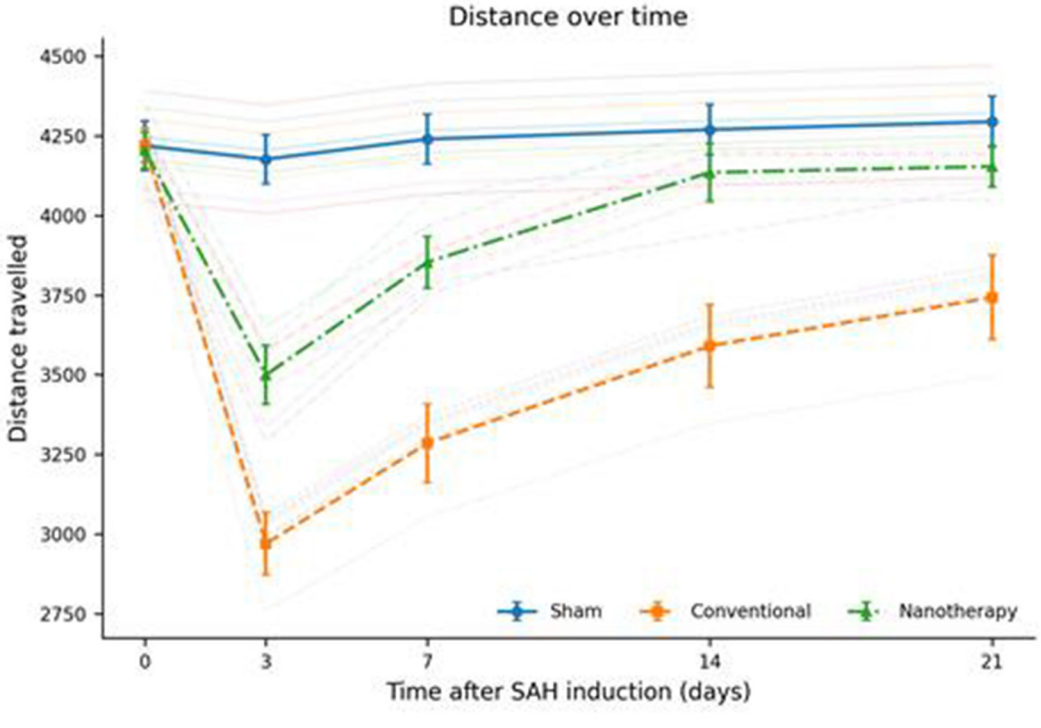


Fig. 8. Changes in total distance travelled following subarachnoid hemorrhage induction

Mean velocity

Mean locomotor velocity showed a comparable recovery pattern (***Fig. 9***). The baseline-adjusted longitudinal model included 99 observations from 26 animals and identified a significant group-by-time interaction (Wald $\chi^2[6] = 7026.43$, $p < 0.001$). At day 21, mean velocity was 14.35 ± 0.39 cm/s in the Sham group, 12.48 ± 0.45 cm/s in the Conventional treatment group, and 13.86 ± 0.28 cm/s in the Nanotherapy group. The mean difference between Nanotherapy and Conventional treatment was 1.38 cm/s. The between-group difference was statistically significant after Holm correction (adjusted $p < 0.001$), with a Hedges' g of 3.57.

Center exploration

Center exploration was reduced following subarachnoid hemorrhage and demonstrated greater recovery in the Nanotherapy group than in the conventional treatment group (***Fig. 10***). The baseline-adjusted generalized estimating equation model included 99 observations from 26 animals and demonstrated a significant group-by-time interaction (Wald $\chi^2[6] = 22469.61$, $p < 0.001$). At day 21, mean center exploration was 42.49 ± 0.95 s in the Sham group, 37.73 ± 1.08 s in the Conventional treatment group, and 41.35 ± 0.61 s in the Nanotherapy group. Nanotherapy increased center exploration by a mean of 3.62 s compared with conventional treatment. The difference remained statistically significant after correction for multiple comparisons (Holm-adjusted $p < 0.001$), with a large standardized effect size (Hedges' g = 4.02).

Immobility

Immobility time demonstrated an inverse treatment response, with persistently higher immobility in animals receiving *conventional* treatment and lower values in the Nanotherapy group (***Fig. 11***). The baseline-adjusted generalized estimating equation model included 99 observations from 26 animals and demonstrated a significant group-by-time interaction (Wald $\chi^2[6] = 2187.03$, $p < 0.001$). At day 21, mean immobility was 36.12 ± 4.01 s in the Sham group, 54.17 ± 6.31 s in the Conventional treatment group, and 40.76 ± 3.29 s in the nanotherapy group. Compared with the Conventional treatment group, the Nanotherapy group reduced immobility by a mean of 13.40 s. The difference remained statistically significant after Holm correction (adjusted $p = 0.002$). The standardized difference was large and favored the Nanotherapy group (Hedges' g = −2.62).

Correlations between neurological and behavioral outcomes

Among the 24 animals with complete assessments at day 21, neurological and open-field outcomes demonstrated strong correlations. Higher modified Garcia and beam-balance scores were associated with greater travelled distance, higher velocity, and greater center exploration, whereas these measures were inversely associated with immobility. Travelled distance and velocity showed particularly strong concordance, indicating that these parameters represented closely related dimensions of locomotor recovery. Similarly, neurological scores covaried with exploratory behavior, supporting the internal consistency of the observed treatment response.

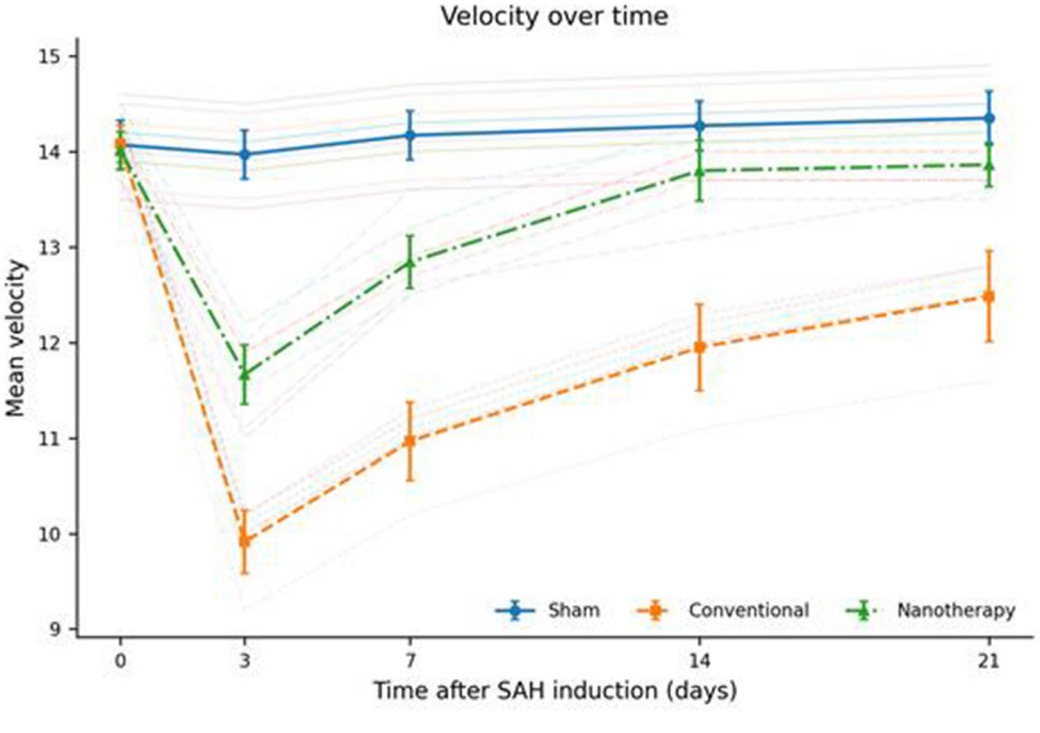


Fig. 9. Changes in mean locomotor velocity following subarachnoid hemorrhage induction

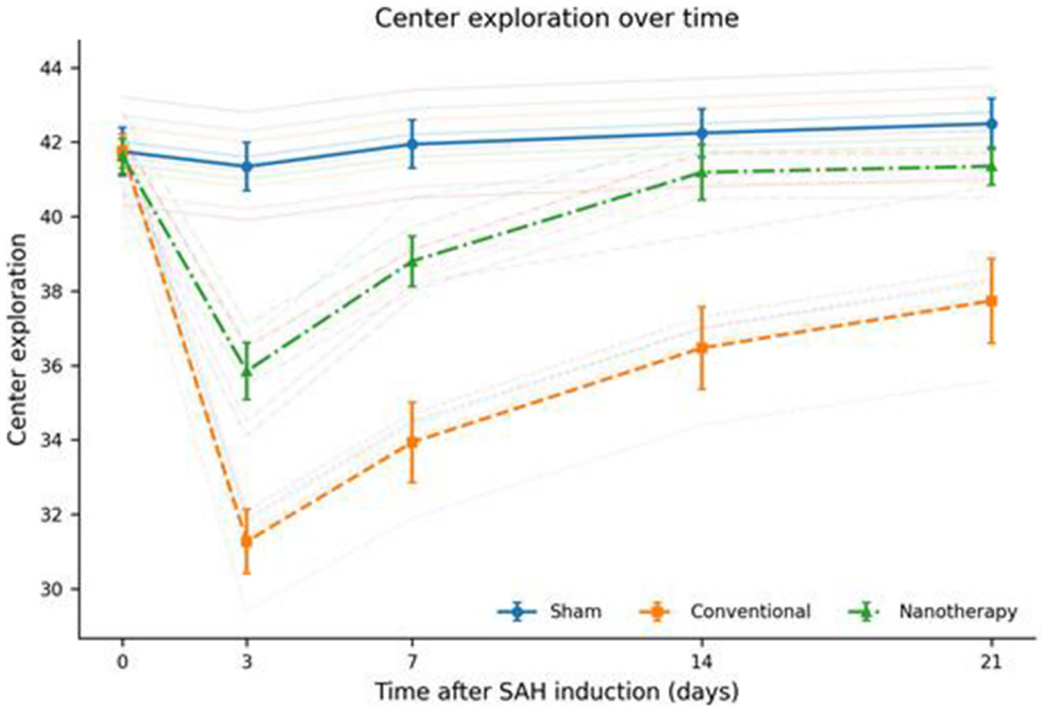


Fig. 10. Changes in center exploration following subarachnoid hemorrhage induction

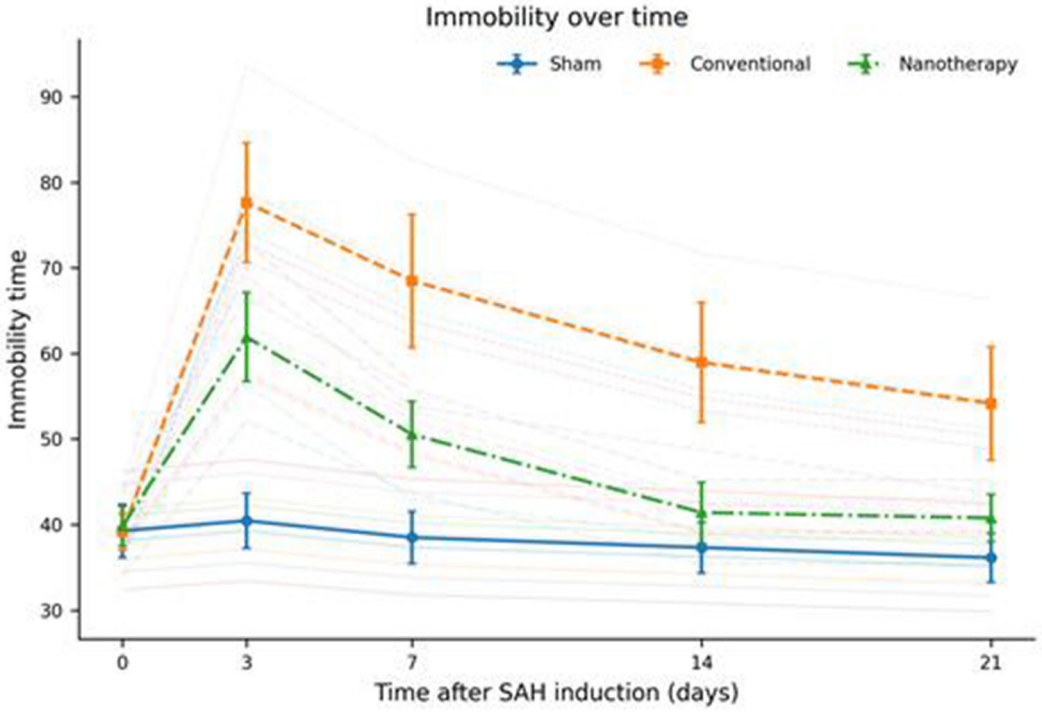


Fig. 11. Time course of immobility following subarachnoid hemorrhage induction

Overall treatment effect

Across the longitudinal analyses, nanotherapy was consistently associated with improved functional recovery compared with Conventional treatment. The treatment effect was observed in neurological performance, beam-balance ability, locomotor activity, center exploration, immobility, and body-weight recovery. The largest and most consistent between-group differences were observed at day 21 for modified Garcia score, beam-balance score, travelled distance, velocity, center exploration, and immobility. Although mortality was numerically lower in the Nanotherapy

group, the study was not sufficiently powered to establish a statistically significant survival benefit. No overt acute adverse reactions temporally associated with intrathecal administration were observed during the study period. Specifically, no treatment-related seizures, respiratory deterioration, abnormal recovery from anesthesia, or immediate procedure-related deaths were recorded. Nevertheless, the study was not designed to identify subclinical, histopathological, biochemical, or delayed toxic effects.

Discussion

The present proof-of-concept study demonstrates that intrathecal administration of cerium oxide nanoparticles significantly improves functional recovery following experimental aSAH. Compared with conventional nimodipine treatment, nanotherapy resulted in improved neurological performance, enhanced motor coordination, increased spontaneous locomotor activity, improved exploratory behavior, and accelerated recovery of body weight throughout the observation period. Although the study was not powered to detect differences in survival, mortality was numerically lower in the Nanotherapy group. Collectively, these findings suggest that local administration of nanoceria may provide clinically meaningful neuroprotection during the early phase of secondary brain injury after SAH.

The importance of these findings extends beyond the observed behavioral improvements. Increasing evidence indicates that long-term neurological outcome after aSAH is determined predominantly by the severity of early brain injury (EBI) rather than angiographic vasospasm alone. EBI comprises a complex interplay of transient global ischemia, blood–brain barrier disruption, oxidative stress, neuroinflammation, mitochondrial dysfunction, and microvascular impairment that develops immediately after aneurysm rupture and precedes delayed cerebral ischemia. Consequently, therapeutic strategies targeting these early pathological processes are increasingly recognized as a priority for improving neurological recovery after SAH [15]. Our findings support this concept by demonstrating that intervention during the acute post-hemorrhagic period translates into sustained functional benefits extending over three weeks.

One of the major strengths of the present study is the emphasis on longitudinal behavioral assessment rather than isolated biochemical measurements. Functional recovery represents one of the most clinically relevant endpoints in experimental cerebrovascular research because it integrates the combined effects of neuronal preservation, vascular function, neuroplasticity, and systemic recovery. Current recommendations for preclinical stroke research emphasize the use of complementary behavioral paradigms to capture different neurological domains instead of relying on a single neurological scale [16]. Accordingly, we combined the modified Garcia neurological score, beam balance testing, automated open-field analysis, body-weight monitoring, and survival assessment. The remarkable consistency of treatment effects across these independent outcome measures substantially strengthens the validity of our observations.

The modified Garcia score demonstrated the most pronounced treatment-related improvement. Because this composite neurological scale simultaneously evaluates spontaneous activity, sensorimotor function, proprioception, balance, and reflex integrity, it is considered one of the most robust tools for assessing global neurological deficits after experimental stroke. Importantly, improvements observed in the Garcia score were paralleled by objective improvements in beam balance performance and automated locomotor analysis, suggesting that the observed neurological recovery reflects genuine restoration of functional capacity rather than isolated improvement in a single behavioral domain.

Automated open-field analysis provided additional evidence supporting enhanced recovery following nanotherapy. Unlike observer-dependent neurological scoring systems, computer-based tracking objectively quantifies locomotor activity and exploratory behavior while minimizing subjective bias. Increased travelled distance, higher locomotor velocity, greater center exploration, and reduced immobility consistently indicated improved functional recovery in the Nanotherapy group. The strong correlations observed between neurological scores and locomotor parameters further support the internal consistency of these behavioral outcomes.

Although the present study was intentionally designed as a functional proof-of-concept investigation, the observed therapeutic effects are biologically plausible considering the unique catalytic properties of cerium oxide nanoparticles. Unlike conventional antioxidants, which are irreversibly consumed after neutralizing reactive oxygen species, nanoceria possess reversible Ce^{3+}/Ce^{4+} redox cycling together with oxygen-vacancy formation, allowing continuous regeneration of their antioxidant activity. This catalytic mechanism enables prolonged scavenging of superoxide radicals, hydrogen peroxide, and other reactive oxygen species without rapid depletion. Furthermore, stabilization of citrate-coated nanoparticles improves their colloidal stability and biological compatibility, facilitating sustained activity in physiological environments.

The neuroprotective potential of cerium oxide nanoparticles has been demonstrated in several neurological disease models. Experimental studies have shown that nanoceria reduce oxidative damage, preserve mitochondrial function, suppress neuroinflammatory activation, decrease neuronal apoptosis, and improve neurological recovery after ischemic stroke and traumatic brain injury [17-18]. Similar mechanisms have also been described in experimental subarachnoid hemorrhage, where catalytic antioxidants have been shown to reduce oxidative injury and improved neurological outcomes. Our findings extend these observations by demonstrating that locally administered nanoceria delivered directly into the cerebrospinal fluid resulted in sustained improvements across multiple independent behavioral endpoints.

An important aspect of the present study is the intrathecal route of administration. Systemic delivery of neuroprotective agents after SAH is limited by impaired blood–brain barrier permeability, systemic metabolism, and dose-dependent adverse effects, particularly hypotension in the case of nimodipine. Intrathecal administration bypasses these limitations by placing the therapeutic agent directly into the cerebrospinal fluid, where pathological blood products accumulate during the earliest phase of injury [19-20]. Previous clinical and experimental studies investigating intrathecal nimodipine have demonstrated the feasibility and

safety of local drug delivery while achieving higher local drug concentrations than systemic administration. The present findings further support the concept that local pharmacological intervention may represent a promising strategy for targeting early brain injury.

Another clinically relevant observation was the improved recovery of postoperative body weight. Weight loss after experimental SAH reflects not only reduced food intake but also the cumulative effects of neurological impairment, systemic inflammation, metabolic stress, and reduced spontaneous activity. Restoration of body weight therefore represents an integrated marker of overall physiological recovery. The faster normalization observed in the nanotherapy group suggests that the beneficial effects of cerium oxide nanoparticles extend beyond isolated neurological function and may reflect broader improvements in systemic recovery.

The present study has several strengths. First, the endovascular perforation model closely reproduces the abrupt arterial rupture, transient intracranial hypertension, and diffuse blood distribution characteristic of aSAH in humans. Second, treatment allocation and behavioral assessment were performed using predefined protocols with blinded outcome evaluation. Third, multiple complementary behavioral paradigms consistently demonstrated similar treatment effects, thereby increasing confidence in the reproducibility of the findings. Finally, the study focused on clinically meaningful functional outcomes rather than isolated molecular endpoints, thereby enhancing its translational relevance.

Several limitations should nevertheless be acknowledged. The present investigation was intentionally designed as a proof-of-concept functional study and therefore did not evaluate the molecular mechanisms responsible for the observed neuroprotection. Histopathological analyses, assessment of oxidative stress biomarkers, inflammatory cytokines, mitochondrial function, blood–brain barrier integrity, and quantitative vasospasm measurements were beyond the scope of the current work. In addition, only a single nanoparticle dose and treatment schedule were investigated, and the observation period was limited to 21 days. Although the formulation was prepared under aseptic conditions using sterile solutions and was visually inspected before administration, batch-specific microbiological sterility testing, quantitative endotoxin assessment, and repeated instrumental measurement of nanoparticle size immediately before injection were not performed. Therefore, the microbiological and physicochemical quality-control procedures should be expanded and validated in subsequent preclinical safety studies. Finally, although survival was numerically improved, the relatively small sample size precluded reliable statistical evaluation of mortality differences.

Future studies should integrate functional assessment with detailed histopathological and molecular analyses to establish causal links between catalytic antioxidant activity and neurological recovery. Evaluation of microglial activation, neuronal survival, oxidative stress markers, cerebrovascular remodeling, and pharmacokinetic properties will provide important mechanistic insights. Furthermore, direct comparison of intrathecal and intravenous administration will help determine the optimal route for clinical translation.

Conclusions

Intrathecal administration of cerium oxide nanoparticles significantly improved functional recovery following experimental subarachnoid hemorrhage compared with conventional nimodipine treatment. Nanotherapy enhanced neurological performance, motor coordination, exploratory behavior, sensorimotor integration, postoperative body weight recovery, and survival compared with conventional treatment. These findings provide proof-of-concept evidence supporting local nanotherapeutic intervention during the early phase of brain injury after aneurysmal subarachnoid hemorrhage. Further mechanistic studies are warranted to determine the molecular pathways responsible for the observed functional benefits and to evaluate the translational potential of this therapeutic strategy.

Disclosure

Conflict of interest statement

The authors declare no conflicts of interest.

Funding

The study was funded by the Ministry of Health of Ukraine using state budget funds as a fragment of research entitled, "Efficacy of Nanostructured Antioxidants Combined with Vasodilators for the Treatment of Combat- and Non-Combat-Related Traumatic and Aneurysmal Intracranial Hemorrhages: An Experimental Study".

References

1. Lauzier DC, Jayaraman K, Yuan JY, Diwan D, Vellimana AK, Osbun JW, Chatterjee AR, Athiraman U, Dhar R, Zipfel GJ. Early Brain Injury After Subarachnoid Hemorrhage: Incidence and Mechanisms. Stroke. 2023 May;54(5):1426-1440. doi: 10.1161/STROKEAHA.122.040072
2. Wang L, Geng G, Zhu T, Chen W, Li X, Gu J, Jiang E. Progress in Research on TLR4-Mediated Inflammatory Response Mechanisms in Brain Injury after Subarachnoid Hemorrhage. Cells. 2022 Nov 26;11(23):3781. doi: 10.3390/cells11233781
3. Kaliuzhka V, Tkachenko A, Myasoedov V, Markevych M, Onishchenko A, Babalyan I, Piatykop V. The Prognostic Value of Eryptosis Parameters in the Cerebrospinal Fluid for Cerebral Vasospasm and Delayed Cerebral Ischemia Formation. World Neurosurg. 2023 May;173:e578-e585. doi: 10.1016/j.wneu.2023.02.096
4. Hänggi D, Beseoglu K, Turowski B, Steiger HJ. Feasibility and safety of intrathecal nimodipine on posthaemorrhagic cerebral vasospasm refractory to medical and endovascular therapy. Clin Neurol Neurosurg. 2008 Sep;110(8):784-90. doi: 10.1016/j.clineuro.2008.05.001
5. Grossen AA, Ernst GL, Bauer AM. Update on intrathecal management of cerebral vasospasm: a systematic review and meta-analysis. Neurosurg Focus. 2022 Mar;52(3):E10. doi: 10.3171/2021.12.FOCUS21629
6. Li X, Han Z, Wang T, Ma C, Li H, Lei H, Yang Y, Wang Y, Pei Z, Liu Z, Cheng L, Chen G. Cerium oxide nanoparticles with antioxidative neurorestoration for ischemic stroke. Biomaterials. 2022 Dec;291:121904. doi: 10.1016/j.biomaterials.2022.121904. Erratum in: Biomaterials. 2024 Sep;309:122612. doi: 10.1016/j.biomaterials.2024.122612
7. Klochkov VK, Malyukin YV, Grygorova GV, Sedyh OO, Kavok NS, Seminko VV, Semynozhenko VP. Oxidation-reduction processes in CeO2-x nanocrystals under UV irradiation. Journal of Photochemistry and Photobiology A: Chemistry. 2018 Sep 1;364:282-7. doi: 10.1016/j.jphotochem.2018.06.025
8. Nikitchenko YV, Klochkov VK, Kavok NS, Karpenko NA, Yefimova SL, Semynozhenko VP, Nikitchenko IV, Bozhkov AI. CeO2 nanoparticles improve prooxidant/antioxidant balance, life quality and survival of old male rats. Biogerontology. 2023 Feb;24(1):47-66. doi: 10.1007/s10522-022-09987-6
9. Jeong HG, Cha BG, Kang DW, Kim DY, Ki SK, Kim SI, Han JH, Yang W, Kim CK, Kim J, Lee SH. Ceria Nanoparticles Synthesized With Aminocaproic Acid for the Treatment of

Subarachnoid Hemorrhage. Stroke. 2018 Dec;49(12):3030-3038. doi: 10.1161/STROKEAHA.118.022631
10. Malyukin Y, Klochkov V, Maksimchuk P, Seminko V, Spivak N. Oscillations of Cerium Oxidation State Driven by Oxygen Diffusion in Colloidal Nanoceria (CeO2 - x). Nanoscale Res Lett. 2017 Oct 13;12(1):566. doi: 10.1186/s11671-017-2339-7
11. Kavok N, Grygorova G, Klochkov V, Yefimova S. The role of serum proteins in the stabilization of colloidal LnVO4: Eu3+ (Ln= La, Gd, Y) and CeO2 nanoparticles. Colloids and Surfaces A: Physicochemical and Engineering Aspects. 2017 Sep 20;529:594-9. doi: 10.1016/j.colsurfa.2017.06.052
12. Sehba FA. Rat endovascular perforation model. Transl Stroke Res. 2014 Dec;5(6):660-8. doi: 10.1007/s12975-014-0368-4
13. Garcia JH, Wagner S, Liu KF, Hu XJ. Neurological deficit and extent of neuronal necrosis attributable to middle cerebral artery occlusion in rats. Statistical validation. Stroke. 1995 Apr;26(4):627-34; discussion 635. doi: 10.1161/01.str.26.4.627
14. Kraeuter AK, Guest PC, Sarnyai Z. The Open Field Test for Measuring Locomotor Activity and Anxiety-Like Behavior. Methods Mol Biol. 2019;1916:99-103. doi: 10.1007/978-1-4939-8994-2_9
15. Lauzier DC, Vinters HV, Magaki SD. Microglia and macrophages in brain injury and repair after subarachnoid hemorrhage. Neural Regen Res. 2026 Jan 1;21(1):308-309. doi: 10.4103/NRR.NRR-D-24-01037
16. Ruan J, Yao Y. Behavioral tests in rodent models of stroke. Brain Hemorrhages. 2020 Dec;1(4):171-184. doi: 10.1016/j.hest.2020.09.001
17. Yuan B, Jiang T, Han J, Zheng T, Wang M. Multiple Applications of Nanomaterials in the Diagnosis and Treatment of Hemorrhagic Stroke. Biomolecules. 2025 Sep 3;15(9):1272. doi: 10.3390/biom15091272
18. Jiang Z, Chen Q, Yang H. Drug delivery strategies for neuroprotective therapy in ischemic stroke: Application of nanotechnology. Neural Regen Res. 2026 May 1;21(5):1793-1808. doi: 10.4103/NRR.NRR-D-24-01383
19. Wang Y, Xu J, Yan W, Zhang S, Luo C, Wang Y. Nanotechnology-donated ischemic stroke therapeutics: evolving strategies from the basic to the cutting-edge. Theranostics. 2026 Jan 1;16(6):3173-3205. doi: 10.7150/thno.127504
20. Zhou D, Fang T, Lu LQ, Yi L. Neuroprotective potential of cerium oxide nanoparticles for focal cerebral ischemic stroke. J Huazhong Univ Sci Technolog Med Sci. 2016 Aug;36(4):480-486. doi: 10.1007/s11596-016-1612-9